Comparison of Coded Modulations for Trellis-Shaped Single-Carrier PSK with PAPR Reduction

Yuuki Nishino and Hideki Ochiai
Department of Electrical and Computer Engineering, Yokohama National University
79-5 Tokiwadai, Hodogaya, Yokohama, Kanagawa 240-8501, Japan
Email: nishino@ochiailab.dnj.ynu.ac.jp, hideki@ynu.ac.jp

***Abstract*— Trellis shaping (TS) is known as a flexible technique that controls a transmit symbol sequence such that the resulting transmitted signals meet a certain desired property. Our recent work has shown that TS can generate a near constant envelope signal for PSK signaling even with strict bandwidth limitation through the use of a near rectangular pulse-shaping filter. In this work, we combine this TS approach with several coded modulation schemes and compare their performances in terms of achievable peak power reduction capability and bit error rate over an AWGN channel.**

I. Introduction

Power and bandwidth efficiencies have been two important factors in wireless communications systems. In general, strictly band-limited signals suffer from high peak-to-average power ratio (PAPR). Linear amplification of high PAPR signals requires a large back-off operation of power amplifier (PA), which results in a considerable penalty in terms of power efficiency. Therefore, there is a trade-off between bandwidth efficiency and power consumption at the transmitter.

Together with frequency-domain equalization, a single-carrier system has been considered advantageous over orthogonal frequency-division multiplexing (OFDM) for communications over frequency-selective fading channels due to its lower PAPR property [1]. However, PAPR can be considerably higher even for single-carrier systems when the signal is severely band-limited (see, e.g., [2] and references therein). Therefore, PAPR reduction schemes play an important role for such single-carrier systems.

The trellis shaping (TS) [3] is a constellation-shaping method that can control symbol sequences by using the structure of convolutional (or trellis) codes, together with the Viterbi algorithm (VA) at the transmitter. Originally, TS was introduced in order to reduce the average power of high-order quadrature amplitude modulation (QAM) signals by controlling symbol sequences. Later, its application to PAPR reduction of a single-carrier system was studied in [4]. Our recent work [5] has revealed that a carefully designed TS is capable of generating near constant envelope for PSK signaling even if a very narrow pulse-shaping filter is employed.

In practice, most digital communication systems are operated with error correcting codes to enhance the robustness against noise and fading. This fact motivates us to investigate the use of error correcting codes in combination with TS. In [6], a serial concatenation of TS and channel coding has been proposed where the TS is considered as an inner code. It has been shown that by using turbo decoding principle, the overall system can achieve near channel capacity performance. The major drawback of such an approach is its increasing signal processing delay due to the iterative decoding process and thus may not be applicable to some real-time applications where a large amount of delay is intolerable.

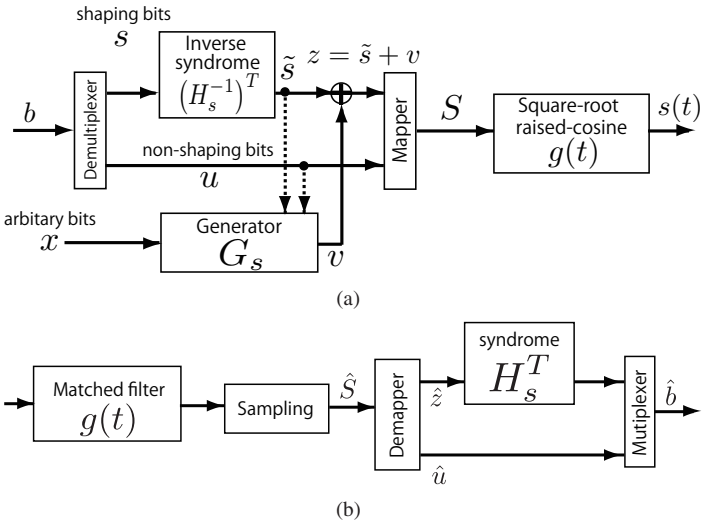

Fig. 1. Receiver of general trellis shaping system model. (a) Transmitter. (b) Receiver.

Therefore, in this paper, we investigate an application of simple coded modulation schemes with low decoding complexity to the TS system in the framework of single-carrier PSK signaling. As an example of coded modulation, we consider trellis coded modulation (TCM) [7], multilevel coding (MLC) [8, 9], and pragmatic trellis coded modulation (PTCM) [10], and evaluate their PAPR reduction capabilities as well as their bit error rate (BER) performances.

II. Trellis Shaping System Model

A general trellis shaping system model is shown in Fig. 1, where $\boldsymbol{G}_s$ is a generator matrix of a convolutional code, $\boldsymbol{H}_s^T$ is the corresponding syndrome former matrix, and $\left(\boldsymbol{H}_s^{-1}\right)^T$ is

978-1-4673-1881-5/12/$31.00 ©2012 IEEE

its left inverse matrix. We assume that $\boldsymbol{G}_s$ is a $1 \times n_s$ matrix and thus $\boldsymbol{H}_s^T$ is a $n_s \times (n_s - 1)$ matrix. The inverse matrix is thus a $(n_s - 1) \times n_s$ matrix. These matrices should satisfy

$$\boldsymbol{G}_s \boldsymbol{H}_s^T = \boldsymbol{O},$$
$$\left(\boldsymbol{H}_s^{-1}\right)^T \boldsymbol{H}_s^T = \boldsymbol{I},$$

where $\boldsymbol{O}$ denotes a zero matrix and $\boldsymbol{I}$ is an identity matrix.

At the transmitter, an input information sequence $\boldsymbol{b}$ is divided into a sequence of shaping bits $\boldsymbol{s}$ and that of non-shaping bits $\boldsymbol{u}$. The shaping bits $\boldsymbol{s}$ are encoded by the left inverse of the syndrome former as

$$\tilde{\boldsymbol{s}} = \boldsymbol{s}\left(\boldsymbol{H}_s^{-1}\right)^T. \tag{1}$$

This shaping process introduces one bit redundancy in $\boldsymbol{s}$ and at this stage, one may add an arbitrary codeword of $\boldsymbol{G}_s$ to $\tilde{\boldsymbol{s}}$. Specifically, $\boldsymbol{v} = \boldsymbol{x}\boldsymbol{G}_s$ can be added in modulo-2 manner to $\tilde{\boldsymbol{s}}$ where $\boldsymbol{x}$ is an arbitrary bit sequence. The sequence $\boldsymbol{z} = \tilde{\boldsymbol{s}} + \boldsymbol{v}$ together with a sequence of non-shaping bits $\boldsymbol{u}$ may determine, based on some bit labeling, the resulting PSK symbol sequence $\boldsymbol{S} = \{S_l, -\infty < l < \infty\}$ to be transmitted. At the receiver, the received estimate symbol sequence $\tilde{\boldsymbol{S}}$ is divided into $\tilde{\boldsymbol{z}}$ and $\tilde{\boldsymbol{u}}$, and the original shaping bits $\boldsymbol{s}$ can be recovered simply by multiplying $\tilde{\boldsymbol{z}}$ with $\boldsymbol{H}_s^T$ since $\tilde{\boldsymbol{z}}\boldsymbol{H}_s^T = \boldsymbol{s}$ as long as $\tilde{\boldsymbol{z}} = \boldsymbol{z}$ [3].

The baseband signal at the transmitter is expressed as

$$s(t) = \sum_{l=-\infty}^{\infty} S_l g(t - lT_s),$$

where T_s is the Nyquist symbol interval and $g(t)$ is the pulse shaping filter. Our objective is to choose $\boldsymbol{v}$ (or $\boldsymbol{x}$) such that the resulting dynamic range of the signal envelope, i.e., $|s(t)|$, has a low peak value.

III. Coded Modulation with TS

We describe the three candidate coded modulation approaches directly applicable to our TS system described in the previous section. Throughout this section, we specifically consider M-ary PSK with $M = 32$ as our example, but the approach is applicable to other systems (such as $M = 16$ and 64) without major modification.

A. TS with Trellis Coded Modulation (TS-TCM)

The proposed TS system combined with TCM (denoted by TS-TCM) is shown in Fig. 2. An input information bit sequence $\boldsymbol{b}$ is divided into shaping bit sequence $\boldsymbol{s}$ and non-shaping bit sequence $\boldsymbol{u}$. The latter is encoded into the coded bit sequence $\boldsymbol{c}$ using a rate-2/3 Ungerboeck TCM code with a S-state encoder. With 32-PSK, each symbol carries $\log_2 32$ = 5 bits and for the lth symbol we denote a shaping bit by $\boldsymbol{s}_l = \left[s_l^0\right]$ and two non-shaping bits by $\boldsymbol{u}_l = \left[u_l^0, u_l^1\right]$. The latter bits are coded by a rate-2/3 TCM and we denote the coded bits by $\boldsymbol{c}_l = \left[c_l^0, c_l^1, c_l^2\right]$. (The relationship between the bits s_l^i, u_l^j, and c_l^k is summarized in Fig. 2(a).) Encoding shaping bit $\boldsymbol{s}_l$ into $\hat{\boldsymbol{s}}_l = \left[\hat{s}_l^0, \hat{s}_l^1\right]$ by (1) and adding $\boldsymbol{v}_l$ to $\hat{\boldsymbol{s}}_l$ (i.e., $\hat{\boldsymbol{s}}_l + \boldsymbol{v}_l = \boldsymbol{z}_l$) at the trellis shaping encoder, we obtain

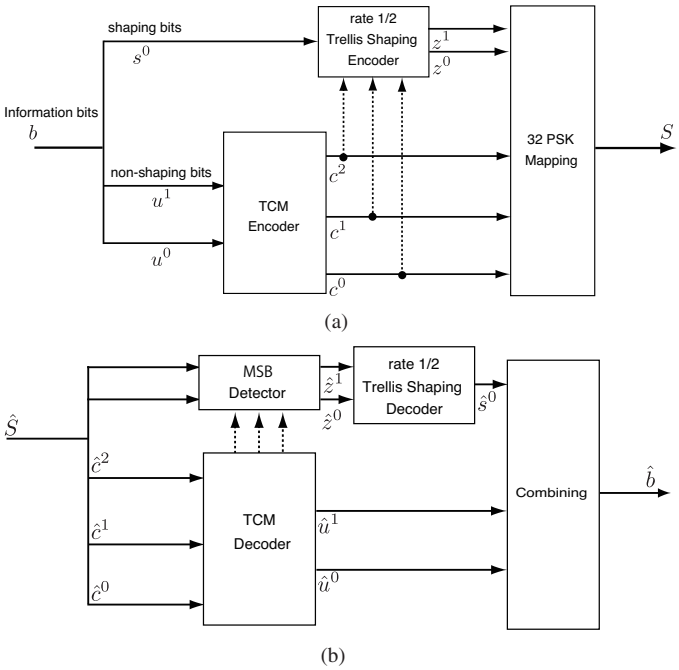

Fig. 2. TS with TCM (TS-TCM) for 32-PSK example. (a) Transmitter. (b) Receiver.

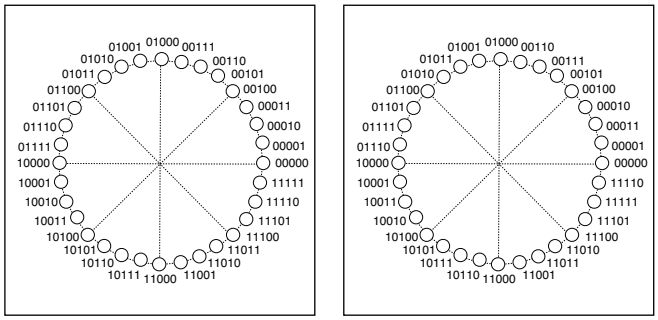

(a) (b)

Fig. 3. Bit labelings of 32-PSK signal constellation. (a) Natural labeling (for TS-TCM and TS-MLC). (b) Labeling proposed in [10] (for TS-PTCM).

a 5-bit vector expressed as $\boldsymbol{Q}_l = \left[Q_l^4, Q_l^3, Q_l^2, Q_l^1, Q_l^0\right] = \left[z_l^1, z_l^0, c_l^2, c_l^1, c_l^0\right]$. This vector $\boldsymbol{Q}_l$ is mapped to a 32-PSK complex symbol S_l as follows:

$$S_l = \xi(\boldsymbol{Q}_l), \quad x_l \in \Omega,$$
$$\Omega = \{e^{j2\pi k/32} : k = 0, 1, \cdots, 31\},$$

where $\xi(\cdot)$ denotes a signal mapping and Ω is the 32-PSK signal set. For TS-TCM, we use the natural labeling defined in Fig. 3(a). This labeling has a large minimum distance property and PAPR controlling capability.

At the receiver, the received symbol $\hat{S}_l$ is expressed as

$$\hat{S}_l = \sqrt{E_s} S_l + N_l, \tag{2}$$

where E_s is the symbol energy and N_l is a complex additive white Gaussian noise (AWGN) with one-sided power spectral density N_0. In this work, we only consider the AWGN channel without fading. An extension to fading channels is

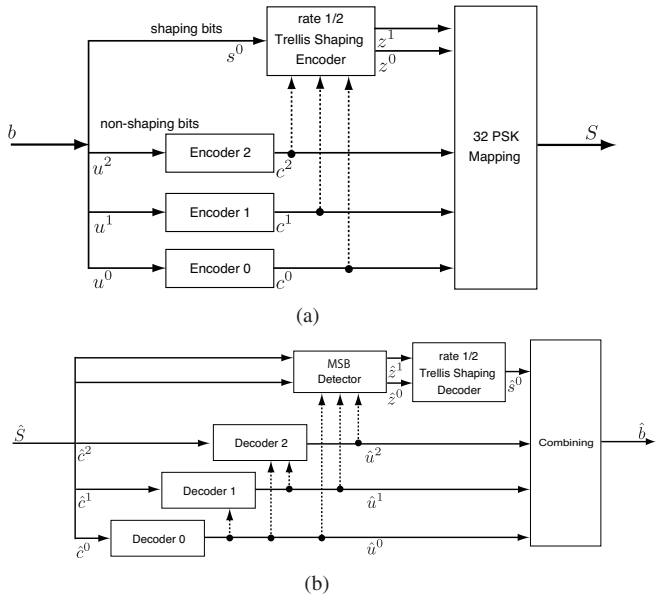

Fig. 4. TS with MLC (TS-MLC) for 32-PSK example. (a) Transmitter. (b) Receiver.

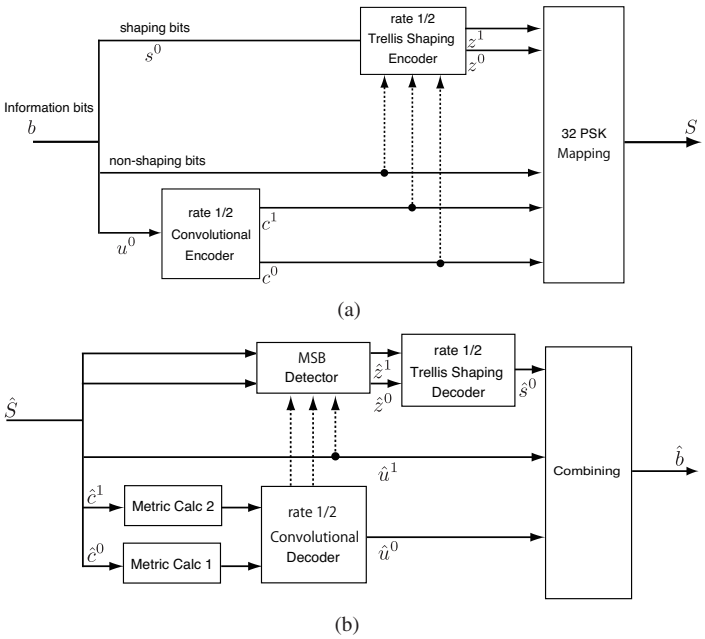

Fig. 5. TS with PTCM (TS-PTCM) for 32-PSK example. (a) Transmitter. (b) Receiver.

straightforward, but the system parameter optimization over general fading channels may be challenging.

Received complex baseband symbol $\hat{S}_l$ is decoded by trellis decoder (maximum-likelihood sequence detector using Viterbi algorithm) [7], and divided into $\hat{\boldsymbol{z}}_l$ and $\hat{\boldsymbol{u}}_l$. The original shaping bits $\boldsymbol{s}_l$ can be recovered from $\hat{\boldsymbol{z}}_{\boldsymbol{l}}$ at trellis shaping decoder.

B. TS with Multilevel Coded Modulation (TS-MLC)

Figure 4 shows the 32-PSK example of the proposed trellis shaping model with MLC (TS-MLC). At the transmitter, input information bit $b = \{b_0, \ldots, b_{L-1}\}$ is divided into shaping bit sequence $\boldsymbol{s} = \left[s^0\right]$ with $s^0 = (s_0^0, \ldots, s_{L^s-1}^1)$, and non-shaping bit sequences $\boldsymbol{u} = \left[u^0, u^1, u^2\right]$ with $u^i = (u_0^i, \ldots, u_{L^i-1}^i)$, where L, L^s, and L^i denote the lengths of information bit sequence, shaping bit sequence, and the ith non-shaping bit sequence, respectively. In the case of 32-PSK, we may express

$$L^s + \sum_{i=0}^{2} L^i = L.$$

Non-shaping bit sequences are encoded into coded bit sequences $\boldsymbol{c} = \left[c^0, c^1, c^2\right]$ with $c^i = (c_0^i, \ldots, c_{N-1}^i)$, where N denotes a codeword length of each binary encoder. Since the shaping bits are uncoded, it follows that $L^s = N$.

Since the total coding rate R of this scheme is equal to the sum of the individual code rate $R^i = L^i/N$, we have

$$R = \frac{L^s}{N} + \sum_{i=0}^{2} R^i = \frac{1}{N}(L^s + \sum_{i=0}^{2} L^i) = \frac{L}{N},$$

where R^i is designed by the capacity rule [9]. For our 32-PSK signaling with 3 information bits per symbol, we numerically found that the coding rates of each level are $R^2 = 1.0$ (uncoded), $R^1 = 0.83 \approx 5/6$, and $R^0 = 0.16 \approx 1/6$.

We use convolutional codes and punctured convolutional codes for each encoder. It is well known that the suitable bit labeling for MLC is a natural labeling depicted in Fig. 3(a) [9].

Received symbols are successively decoded by corresponding decoders based on multi-stage decoding (MSD). At the ith decoding stage, the decoder processes not only the received symbol sequence $\hat{\boldsymbol{S}}$, but also the decisions $\hat{u}^j$, where $j = 0, \ldots, i-1$, made by all the previous decoders. The most significant bits (MSBs) ($\hat{z}^j$) can then be detected considering decoded shaping bit sequence $\hat{u}$ as shown in Fig. 4(b).

C. TS with Pragmatic Trellis Coded Modulation (TS-PTCM)

The proposed system model based on 32-PSK pragmatic trellis coded modulation (TS-PTCM) is shown in Fig. 5. Similar to the TS-TCM scheme, an input information bit sequence is divided into sequences $\boldsymbol{s}_l = \left[s_l^0\right]$ and $\boldsymbol{u}_l = \left[u_l^0, u_l^1\right]$ at the transmitter. The least significant bit (LSB) of non-shaping bit sequence u_l^0 is fed into rate-1/2 convolutional encoder, resulting in a coded bit sequence $\boldsymbol{c}_l = \left[c_l^0, c_l^1\right]$ as shown in Fig. 5(a). The transmitted symbol can then be expressed as $\boldsymbol{Q}_l = \left[z_l^1, z_l^0, u_l^1, c_l^1, c_l^0\right]$.

We use a bit labeling which has equally spaced signal points for any combinations of $\boldsymbol{c}_l$ [10]. For example, in the case of rate-1/2 encoder, there are 4 patterns of $\boldsymbol{c}_l$ as $[0,0], [0,1], [1,0], [1,1]$. In the 32-PSK signal set of TS-PTCM scheme, the number of the signal subsets that have the same $\boldsymbol{c}_l$ is 8. The resulting constellation is shown in Fig. 3(b). We refer to this bit labeling as a PTCM labeling.

At the receiver, the received symbol is passed through a

TABLE I

THE OPTIMUM PARAMETERS FOR $n_s = 2$ WITH 32-PSK [11].

$\boldsymbol{G}_s$	$\begin{bmatrix} 1+D^2+D^3 & D^2 \end{bmatrix}$
$\boldsymbol{H}_s^T$	$\begin{bmatrix} D^2 \\ 1+D^2+D^3 \end{bmatrix}$
$(\boldsymbol{H}_s^{-1})^T$	$\begin{bmatrix} 1+D & 1 \end{bmatrix}$

TABLE II

THE GENERATOR POLYNOMIALS h_i AND DECODING STATES IN OCTAL FORMAT OF UNGERBOECK TCM CODES ($S = 4, 64$) [7].

Rate	State	h_0	h_1	h_2
2/3	4	5	2	0
	64	103	030	066

bit metric generator. Let λ denote a PTCM bit metric. It can be expressed using a conditional probability density function $P(\cdot|\cdot)$ as

$$\begin{aligned}\hat{\lambda}(c_l^i = d) &= \log P(\hat{S}_l | c_l^i = d) \\ &\approx \log \sum_{x \in \mathcal{X}_d^i} P(\hat{S}_l | x) \\ &\approx \min_{x \in \mathcal{X}_d^i} \left| \hat{S}_l - \sqrt{E_s} x \right|^2, \;\; i = 0, 1; \; d = 0, 1\end{aligned}$$

where the signal subset $\mathcal{X}_d^i$ consists of $\{\xi([\hat{z}_l^1, \hat{z}_l^0, \hat{u}_l^1, c_l^1, c_l^0])\}$ with the ith coded bit c_l^i having a binary value d (i.e., $c_l^i = d$). In the case of 32-PSK, the cardinality of each subset $\mathcal{X}_d^i$ is 16, and 4 bit metrics corresponding to $\{c_l^1, c_l^0\}$ are generated. The bit metrics are used for decision on transmitted symbol sequence with Viterbi decoding. Finally, the MSBs are detected in MSB detector similar to TS-MLC.

IV. SIMULATION RESULTS

In this section, we evaluate the performance of the proposed TS with MLC, TCM, and PTCM in terms of PAPR reduction capability and BER performance through computer simulations. In all the simulation results with trellis shaping, we employ 32-PSK.

A. Simulation Setting

We choose the duration of the impulse response K_s that is used for signal shaping as 12 symbols. Therefore, the number of external memories of TS encoder is chosen as m_{ex}=11. By adding m_{ex} external memories, we can jointly consider the present symbol and the past m_{ex} symbols for codeword selection in the TS encoder. The coding rate of TS encoder is $1/2\,(n_s = 2)$ which has $\nu = 3$ memories with m_{ex} external memories. The limiter method [5] with a threshold parameter $p_{max} = 1.33$ is used for branch metric calculation. See [5] for details of these parameter settings. The roll-off factor of square-root raised-cosine filter used for pulse shaping is set to $\alpha = 0.1$. For the bit labelings considered in this paper, we have found the set of optimal shaping matrices $\boldsymbol{G}_s$, $\boldsymbol{H}_s^T$, and $\left(\boldsymbol{H}_s^{-1}\right)^T$ through computer search [11]. This set is listed in Table I, where D represents a delay element.

TABLE III

THE GENERATOR POLYNOMIALS g_i, DECODING STATES ($S = 4, 64$), AND PUNCTURING TABLE OF CONVOLUTIONAL CODES IN OCTAL FORM.

Rate	State	g_1	g_2	g_3	g_4	g_5	g_6
1/2	4	5	7	-	-	-	
	64	133	171	-	-	-	-
1/6	4	7	7	7	7	5	5
	64	173	151	135	135	163	137

Rate	State	g_1	g_2	Puncturing table
5/6	4	5	7	1 0 1 1 1 1 1 0 0 0
	64	133	171	1 1 0 1 0 1 0 1 0 1

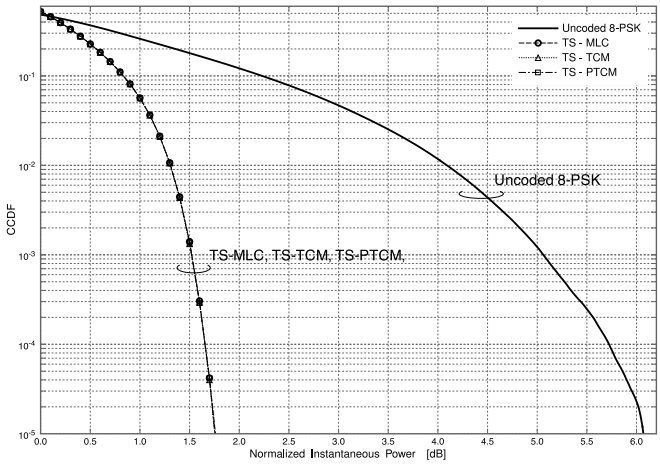

Fig. 6. Comparison of PAPR reduction performances between TS-CM (TS-TCM, TS-MLC, TS-BICM) 32-PSK and uncoded 8-PSK.

For an encoder of the convolutional codes for error correction, we evaluate two scenarios with different number of trellis states, i.e., S = 4 and 64. We have compared the simulation results of 32-PSK with the three coded modulation approaches (simply denoted by TS-CM), trellis-shaped 16-PSK (without channel coding), and uncoded 8-PSK (without shaping). Note that these cases are chosen as references since they have the same number of information bits per PSK symbol (i.e., 3 information bits per symbol). Note also that as we mentioned in Section III-B, in the case of TS-MLC, two binary convolutional codes with rates $R^1 = 5/6$ and $R^2 = 1/6$ are used whereas a single binary convolutional code with rate $R = 1/2$ is used for TS-PTCM. The parameters of the convolutional codes used in our simulations (i.e., coding rates, generator polynomials, and puncturing tables) are listed in Tables II and III.

B. Peak Power Reduction Performance

Figure 6 compares the complementary cumulative distribution function (CCDF) of the instantaneous power (normalized by the average power) for several TS-CM as well as that without TS. Peak power reduction of more than 3.5dB is

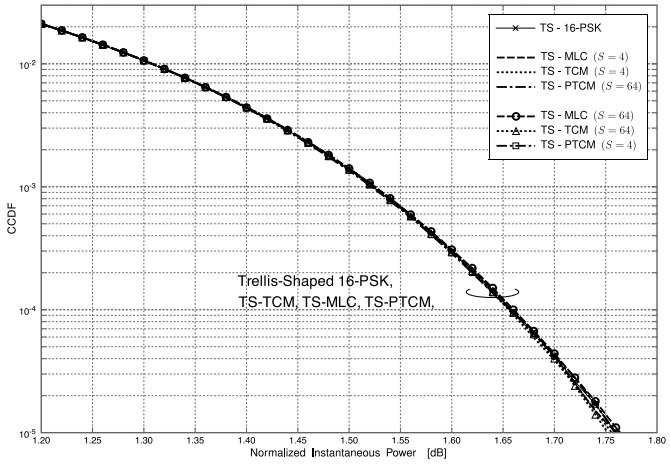

Fig. 7. Comparison of PAPR reduction performances of TS-CM (TS-TCM, TS-MLC, TS-BICM) 32-PSK with different encoder states ($S = 4, 64$).

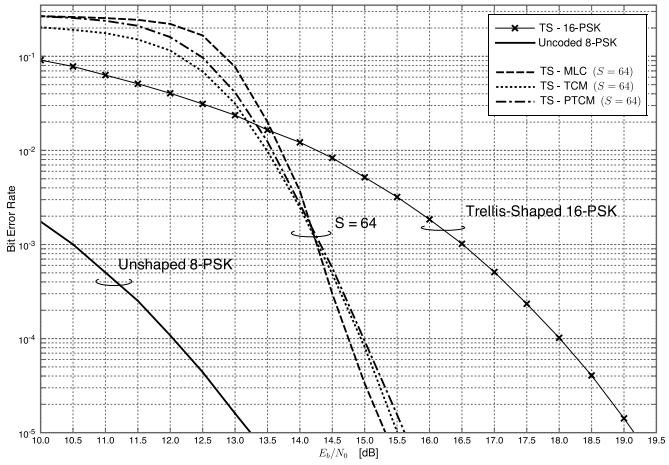

Fig. 8. BER performances of TS-CM ($S = 64$), TS-16PSK, and uncoded 8-PSK.

observed at CCDF of 10^{-3} in the case of TS-CM compared to that without TS (uncoded 8-PSK). It is also observed that the CCDF curves of the three TS-CM cases are almost indiscernible.

To give a closer look at the CCDF performance in the case of TS-CM, Fig. 7 compares the CCDF performances of the TS-TCM, TS-MLC, and TS-PTCM with different channel encoder states ($S = 4, 64$). We can observe that there is no noticeable difference in CCDF performances between different encoder states. Hence, with our labeling design, the number of states in the channel coding and types of CM do not make a difference in terms of peak power reduction performance.

C. BER Performance Comparison

The BER performances of 32-PSK TS-CM with encoder state ($S = 64$) together with those without TS or coding over an AWGN channel are compared in Fig. 8 with respect to E_b/N_0, where E_b is the signal energy per information bit. At a BER of 10^{-5}, all the TS-CM approaches outperform the trellis-shaped 16-PSK without coding by 3.5-3.8 dB in terms of required signal-noise ration (SNR). When we compare the three CM approaches, we observe that for low SNR region, TS-TCM performs best while TS-MLC eventually outperforms the others as SNR increases. If we compare the 32-PSK TS-CM with uncoded 8-PSK, the TS-CM systems still have some gap (about 2 dB at BER of 10^{-5}) in terms of required SNR. However, the benefit of peak power reduction may be more desirable than the required SNR margin in some systems (such as battery-driven terminals) where the PA efficiency is of primary concern. More elaborate system-level evaluation considering PA nonlinearity is required before concluding which approach is advantageous.

V. Conclusion

In this paper, we have investigated a TS system with coded modulation and compared the peak power reduction performance and the BER performance over an AWGN channel. The three TS-CM schemes are introduced and it has been shown that they exhibit similar peak power reduction capability with a significant coding gain. In terms of BER performances, TS-TCM performs better than the others for a low SNR region while TS-MLC outperforms the others for a high SNR region.

For our future work, the performance of the proposed system over frequency-selective fading channels with frequency domain equalization will be investigated.

Acknowledgement

This work was supported in part by MEXT KAKENHI 23686058.

References

[1] D. Falconer, S. Ariyavisitakul, A. Benyamin-Seeyar, and B. Eidson, "Frequency domain equalization for single-carrier broadband wireless systems," *IEEE Commun. Mag.*, vol. 40, no. 4, pp. 58–66, April 2002.

[2] H. Ochiai, "Exact and approximate distributions of instantaneous power for pulse-shaped single-carrier signals," *IEEE Trans. Wireless Commun.*, vol. 10, pp. 682–692, February 2011.

[3] G. D. Forney, Jr. "Trellis shaping,"*IEEE Trans. Inform. Theory*, vol. 38, pp. 281–300, March 1992.

[4] I. S. Morrison,"Trellis shaping applied to reducing the envelope fluctuation of MQAM and band-limited MPSK," in *Proc. Int. Conf. Digital Satellite Commun. (ICDSC'92)*,pp. 143–149, May 1992.

[5] M. Tanahashi and H. Ochiai, "Near constant envelope trellis shaping for PSK signaling." *IEEE Trans. Commun.*, vol. 57, no. 2, pp. 450–458, February 2009.

[6] M. Tanahashi and H. Ochiai, "Turbo decoding of concatenated channel coding and trellis shaping for peak power controlled single-carrier systems," *IEEE Trans. Commun.*, vol. 58, no. 1, pp. 9-15, January 2010.

[7] G. Ungerboeck, "Channel coding with multilevel/phase signals," *IEEE Trans. Inform. Theory*, vol.IT-28, pp.55-67, January 1982.

[8] H. Imai and S. Hirakawa, "A new multilevel coding method using error correcting codes," *IEEE Trans. Inform. Theory*, vol. 23, pp. 371–377, 1977.

[9] U. Wachsmann, R. F. H. Fischer, and J. B. Huber, "Multilevel codes: Theoretical concepts and practical design rules," *IEEE Trans. Inform. Theory*, vol. 45, pp. 1361 - 1391, July 1999.

[10] A. J. Viterbi, J. K. Wolf, E. Zehavi, and R. Padovani, "A pragmatic approach to trellis-coded modulation" *IEEE Commun. Mag.*, vol.27, pp.11-19, July 1989.

[11] Y. Nishino, M. Tanahashi, and H. Ochiai, "A bit-Labeling design for trellis-shaped single-carrier PSK with PAPR reduction," *EURASIP J. Advances in Signal Processing*, vol. 2011.